Localization of Cortical Oscillations Induced by SCS Using Coherence

Lukáš SVOBODA[1], *Andrej STANČÁK*[2], *Pavel SOVKA*[1]

[1]Dept. of Circuit Theory, Czech Technical University, Technická 2, 166 27 Prague 6, Czech Republic
[2]Dept. of Normal, Pathological and Clinical Physiology, Third Faculty of Medicine, Ke Karlovu 4, 120 00 Prague 2, Czech Republic

svobol4@fel.cvut.cz, sovka@fel.cvut.cz, stancak@lf3.cuni.cz

Abstract. *This paper suggests a method based on coherence analysis and scalp mapping of coherence suitable for more accurate localization of cortical oscillations induced by electric stimulation of the dorsal spinal cord (SCS), which were previously detected using spectral analysis. While power spectral density shows the increase of power during SCS only at small number of electrodes, coherence extends this area and sharpens its boundary simultaneously. Parameters of the method were experimentally optimized to maximize its reliability. SCS is applied to suppress chronic, intractable pain by patients, whom pharmacotherapy does not relieve. In our study, the pain developed in lower back and lower extremity as the result of unsuccessful vertebral discotomy, which is called failed-back surgery syndrome (FBSS). Our method replicated the results of previous analysis using PSD and extended them with more accurate localization of the area influenced by SCS.*

Keywords

Magnitude squared coherence, *z*-coherence, failed-back surgery syndrome, spinal cord stimulation, induced oscillations, EEG.

1. Introduction

Failed back surgery syndrome (FBSS) develops as the consequence of unsuccessful back surgery, causing intractable chronic neuropathic pain in lower back and legs, which is, in most cases, resistant to pharmacotherapy [3].

Today, a combination of electric stimulation of dorsal spinal cord (spinal cord stimulation – SCS) and chemical analgesics is applied to alleviate the pain in FBSS. More information about the pain classification, analgesia and SCS is to be found in [5].

In the first part of the research, the detection of induced cortical oscillations was performed [5]. Following successful results, the area influenced by stimulation should be localized more precisely, by request of doctors.

The description of the method is stated in this paper. Analogous to the first part, the interest is focused on the optimal selection of values of parameters required for computation of coherence. Scalp mapping of the coherence values and comparison to the PSD maps is essential part of the method.

2. Patients and EEG Data

The EEG data were recorded from ten FBSS patients, suffering from intractable neuropathic pain located in their lower back and extremity after unsuccessful back surgery. Because the pain did not respond to pharmacological treatment, an electric stimulation of dorsal spinal cord was used for its suppression. The list of the patients, who participated the study, and the conditions of the data measurement and pre-processing are shown in [5].

3. Method

While the difference of power spectral densities during the stimulation and without it expresses the size of power change, coherence helps us to evaluate, how strong the correlation between two electrodes is. Localization of the whole area of scalp showing increased oscillatory activity during ongoing SCS consists of three steps:

1. selection of the reference electrode (based on the results of the first part of the experiment described in [5]),
2. computation of coherences and *z*-coherences between the reference electrode and all other leads in each patient,
3. visualization of the coherence and z-coherence using pseudocolor scalp maps and comparison to PSD difference maps.

3.1 Coherence between Leads

Coherence is a measure of linear coupling between two signals at a given frequency. In our case, the changes of coherence among the leads during SCS on and SCS off

respectively show which electrodes correlate with other leads and how strong the correlation is.

There are 6105 possible pairs for 111 measuring electrodes. Visual analysis of such a large number of frequency courses would be problematic. Fortunately, a major part of the combinations is unimportant for the analysis.

To minimize the number of pairs, in each patient one reference electrode was chosen, where the difference between PSD without SCS and PSD with SCS was maximal at the stimulation frequency (or closely adjacent frequencies).

The coherences were computed between select reference electrode and each of the 110 leads, namely in each patient for all four EEG recordings (unipolar and spatially filtered data, both with and without the stimulation respectively). That way, 4400 frequency courses of coherence were obtained in total, 4×110 for each patient.

3.1.1 Coherence Estimate

We need two smoothed PSD estimates $\hat{S}_x[m]$ and $\hat{S}_y[m]$ for the computation of the estimate of coherence between two random signals $x[m]$ and $y[m]$. It is impossible to compute coherence from unsmoothed power spectra, thus, having just one realization from each signal, it is necessary to use one of smoothing methods.

Besides PSD estimate of each signal, also the estimate of cross power spectrum has to be known. It can be computed using equation [1], [4]

$$\hat{S}_{xy}[m] = \frac{T}{N} \sum_{k=0}^{K-1} X_k^*[m] \cdot Y_k[m] \tag{1}$$

where T is a length of sampling period, N is a total number of samples of each input sequence, K is a number of segments, $Y_k[m]$ is a partial modified periodogram of k-th segment of the signal $y[m]$ and $X^*_k[m]$ is a partial modified periodogram complex conjugated to the periodogram of the corresponding segment of $x[m]$. Both periodograms can be computed using equation [1], [4]:

$$\hat{S}_k[m] = \frac{1}{W} \frac{T}{L} \left| \sum_{l=0}^{L-1} x[l+kL] \cdot w[l] \cdot \mathrm{e}^{-\frac{\mathrm{j}2\pi ml}{L}} \right|^2, \quad k \in \langle 0, K-1 \rangle, \; K = \frac{N}{L}, \tag{2}$$

where the input sequence $x[n]$ of the length N is divided into K successive segments $x_k[l]$, each L samples long, $w[l]$ is a smooth window of the length L, $x[l+kL]$ is the realization of $x_k[l]$ and

$$W = \frac{1}{L} \sum_{l=0}^{L-1} w^2[l]. \tag{3}$$

Consistent estimate of (complex) coherence is to be computed using equation [1]

$$\hat{\gamma}_{xy}[m] = \frac{\hat{S}_{xy}[m]}{\sqrt{\hat{S}_x[m] \cdot \hat{S}_y[m]}} \tag{4}$$

where $\hat{S}_{xy}[m]$ is estimated from equation (1) and $\hat{S}_x[m]$, $\hat{S}_y[m]$ according to

$$\hat{S}_i[m] = \frac{1}{K} \sum_{k=0}^{K-1} \hat{S}_k[m]. \tag{5}$$

The coherence defined by equation (4) is a complex value, but simple and inspectional indicators are required in medical research. That's why, instead of complex coherence, magnitude squared coherence (called just coherence in following text) was used:

$$|\hat{\gamma}_{xy}[m]|^2 = \frac{|\hat{S}_{xy}[m]|^2}{\hat{S}_x[m] \cdot \hat{S}_y[m]}, \; |\hat{\gamma}_{xy}[m]|^2 \in \langle 0, 1 \rangle \tag{6}$$

It is a module of $\hat{\gamma}_{xy}[m]$ taking the value from zero for no coupling between $x[m]$ and $y[m]$ to one for total coupling between these signals.

3.1.2 Transformation to *Z*-coherence

The values of $|\hat{\gamma}_{xy}[m]| = \sqrt{|\hat{\gamma}_{xy}[m]|^2}$ are not of normal distribution, which is an assumption of figure of methods used for further analysis.

According to empirical knowledge, for the values of the estimate $|\hat{\gamma}_{xy}[m]| \in \langle 0.35, 0.95 \rangle$, computed from the estimate of PSDs received by smoothing of at least 20 segments, a transformation can be performed using equation [1], [4]

$$\hat{Z}_{xy}[m] = \frac{\sqrt{K-2}}{2} \ln \frac{1 + |\hat{\gamma}_{xy}[m]|}{1 - |\hat{\gamma}_{xy}[m]|} = \sqrt{K-2} \cdot \operatorname{arg\,tanh} |\hat{\gamma}_{xy}[m]| \tag{7}$$

where ln is natural logarithm. The value $\hat{Z}_{xy}[m]$ is approximately normally distributed with mean $\mu_{\hat{Z}}[m] \doteq Z_{xy}[m] + \frac{1}{\sqrt{K-2}}$ and variance $\sigma^2_{\hat{Z}} \doteq 1$. In medicine, it is called z-coherence and used in general instead of magnitude squared coherence estimated using equation (6).

3.2 Limits of Statistical Significance

3.2.1 Computation of the Limit of Statistical Significance of Coherence Used in Medicine

For the analysis of clinical data, it is crucial to know a limit of statistical significance of coherence. Thus, medical sources often recommend using of the significance bound according to [2]

$$|\hat{\gamma}_{xy}|^2_{\min} = 1 - \alpha^{\frac{1}{K-1}} \tag{8}$$

where K is a number of segments used for the coherence computation and α is a significance level. The bound $|\hat{\gamma}_{xy}|^2_{\min}$ is equal at all frequencies. If the value of $|\hat{\gamma}_{xy}[m]|^2$ exceeds this limit at some frequency, it can be taken as statistically significant.

3.2.2 Computation of the Limit of Statistical Significance for *Z*-coherence

The limit of significance for *z*-coherence is given by equation [4]

$$Z_{xy\,\min}[m] = \hat{Z}_{xy}[m] - \frac{1}{\sqrt{K-2}} + u_{1-\alpha} \qquad (9)$$

where $u_{1-\alpha}$ is a fractile of standard normal distribution $N(0,1)$ at significance level $1 - \alpha$. It is evident that, compared to the bound defined by equation (8), the values of bound according to (9) are different at distinct discrete frequencies m.

Besides these two bounds of statistical significance, which are usually used in medical research, also classic, two-tailed confidence intervals can be computed for both coherence and *z*-coherence as shown in Appendix 6.2.

3.3 Parameters of Computation

Coherence is computed from power spectral densities, whose required properties are discussed in [5]. Except the request of narrow confidence interval that is, by coherence, replaced by the limit of statistical significance, the same requirements can be either used in case of coherence.

Thus, it is in need of:

- high frequency resolution;
- low "leakage" between adjacent correlation coefficients;
- non-integer components suppression.

As it was mentioned, coherence could not be computed using unsmoothed power spectra. The higher is a figure of segments entering averaging, the more accurately coherence represents real correlation between single "spectral lines" of input signals. The limit of statistical significance, which must be exceeded to consider the coherence to be significant, decreases at the same time.

3.3.1 Selection of Parameters

The sampling frequency $f_s = 1024$ Hz was given by input signals, the overlap, the number of FFT points and weighting window were used the same way as in power spectra computation that provided identical frequency resolution.

Only the recordings filtered using spatial Laplace operator [6] can be used for coherence computation, because the filtration damps such part of the signal, which is common to all leads (e.g. synchronous components of EEG, external noise). Unipolar (spatially unfiltered) data are unsuitable for coherence analysis, because the common signal is of high amplitude and thus the leads always show strong correlation, namely both by SCS and without SCS.

The level of significance was chosen lower than for spectral analysis ($\alpha = 0.01$), because it cannot be expected that even filtered data is completely independent. That's why there is always some level of coherence unrelated to external effects, e.g. stimulation. In addition, lower value of α decreases the probability of the state that random correlations of power spectra are incorrectly thought as significant.

Each reference lead, towards which coherences of other electrodes are computed, was selected as the electrode, which shows the highest power difference at stimulating frequency (between the PSD with SCS on and PSD with SCS off respectively). The way of detection of these electrodes is described in [5] and their numbers recapitulated in Tab. 1.

Patient No.	A01	A02	A03	A04	A05
Ref. Electrode No.	50	50	37	50	38
Patient No.	A06	A07	A08	A09	A10
Ref. Electrode No.	51	50	37	50	77

Tab. 1. Electrodes used as reference for computation of coherence and *z*-coherence.

4. Results

4.1 Frequency Courses of Coherence and *Z*-coherence

In Fig. 1 the coherences and *z*-coherences computed from EEG signals filtered using Laplace operator method are shown. The coherence by the SCS on is drawn in red, the blue line represents coherence with SCS off and the green dashed line is a limit of statistical significance. Statistically significant coherence between electrodes 64 and 50 (patient A01) and 50 and 37 (patient A08) at stimulation frequency is evident in all pictures.

If coherence and *z*-coherence courses are compared to each other, the main practical differences are higher dynamic of lower values of *z*-coherence and the significance limit, which, by *z*-coherence, is stricter.

4.2 Surface Maps of Difference of Coherences and of Difference of *Z*-coherences

In Fig. 2, there are scalp maps of difference between power spectra during the SCS and without SCS and maps of difference of coherences during SCS-on and SCS-off phases at measured stimulation frequency and two closest adjacent frequencies.

Fig. 2a shows PSD maps of patient A08 for comparison to Fig. 2b with difference of *z*-coherence maps

of the same patient at the same frequency. The *z*-coherence value of the reference lead (electrode 37) was linear interpolated using two nearest electrodes. The values of difference of *z*-coherences under the limit of statistical significance were set to zero.

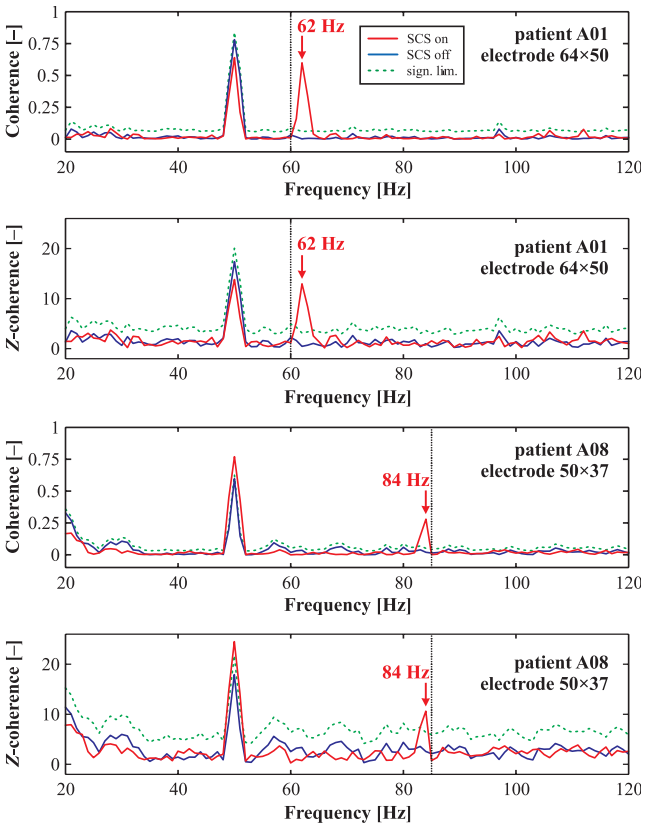

Fig. 1. Selected examples of coherence and z-coherence frequency courses – patients A01 and A08

Coherence and *z*-coherence, compared to PSD, give us more accurate information about the localization of the area, where induced cortical oscillations occur. Frontal part of the red marked field of high correlation in Fig. 2b corresponds with the area of high power increase in Fig. 2a. Besides this, in coherence, strongly correlated electrodes can also be observed at the edge of the main area, which is, thus, much better bounded than at the map of power spectral density.

While the PSD map shows the power increase only at electrode 37, in the *z*-coherence map, there are cortical oscillations induced by SCS apparent also at dorsally placed leads. At PSD maps, these parts are visible just as indistinct yellow and light orange areas.

In Fig. 2c–d, there are surface maps computed by averaging of the maps of difference of coherences (c), *z*-coherences (d) and PSDs (e) of all ten patients. To perform the computation correctly, it was necessary to average maps created in reference to one electrode. The lead 50 was selected as the reference.

Just as average maps of difference of PSDs, also the average maps of difference of coherences show that cortical oscillations induced by spinal stimulation have, in all patients, very similar localization in central area of the scalp. But, in addition, coherence and *z*-coherence give us more accurate idea of position, size and borders of the areas, which are influenced by oscillations induced by spinal cord stimulation.

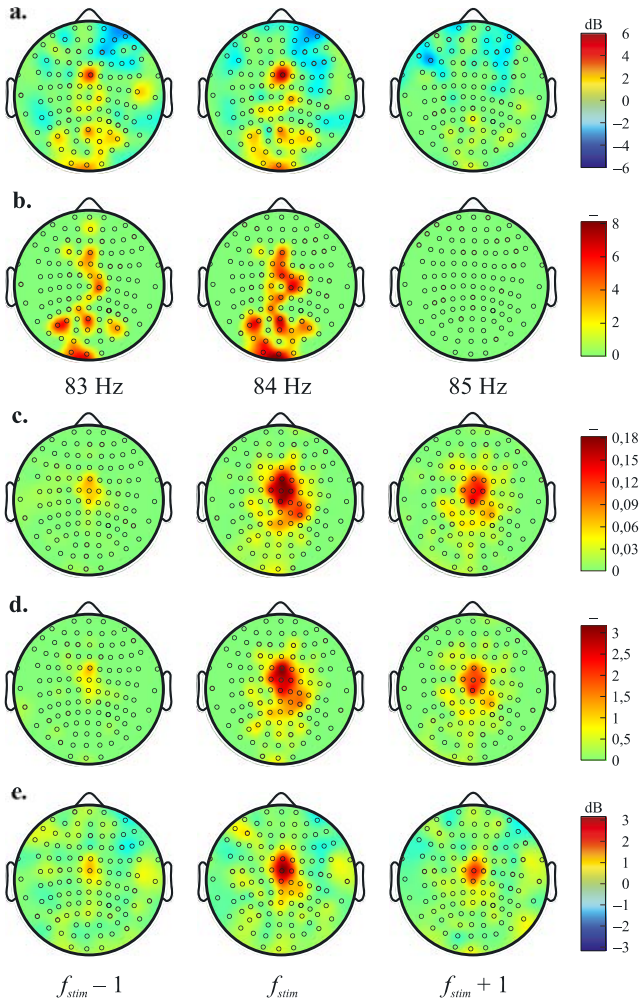

Fig. 2. Scalp maps of difference between SCS-on and SCS-off phases: power spectral density (a) and z-coherence (b) of patient A08; all patients grand average of coherence (c), z-coherence (d) and power spectral density (e).

5. Conclusion

The method described in this paper was successfully used to localize manifestation of induced cortical oscillations on the scalp from EEG. The method was used for the first time for this purpose.

The results proved that induced oscillations in primary sensomotoric cortex related to legs come up as the effect of electrical stimulation of dorsal spinal cord. Statistically significant coherence at stimulation frequency (or its harmonic or subharmonic frequency) on electrodes in central and dorsal part of the scalp was found during SCS.

Our method may be used for precise localization of induced electrical activity in EEG signal, which was previously detected by spectral analysis or another method that provides selection of reference electrode. Magnitude squared coherence and z-coherence, both combined with limit of statistical significance and pseudocolor scalp visualization are reliable tools, which can easily show significant change of correlation between electrodes.

Our method proved the results of previous analysis using PSD and replenished them with more accurate localization of the area influenced by SCS.

6. Appendix

6.1 Derivation of Limit of Statistical Significance for *Z*-coherence

A limit of statistical significance is nothing else than one-tailed (upper) confidence interval. Because of the fact that *z*-coherence is approximately of normal distribution with parameters $\mu_{\hat{Z}}[m] \doteq Z_{xy} + \frac{1}{\sqrt{K-2}}$ and $\sigma_{\hat{Z}} \doteq 1$ [1], the statistic

$$W[m] = \frac{\hat{Z}_{xy}[m] - \mu_{\hat{Z}}[m]}{\sigma_{\hat{Z}}} \tag{10}$$

is of a standard normal distribution $N(0,1)$. The *z*-coherence is statistically significant, if $W[m] \geq u_\alpha$. Introducing into (10), we have

$$\hat{Z}_{xy}[m] - Z_{xy}[m] - \frac{1}{\sqrt{K-2}} \geq u_\alpha \tag{11}$$

and after rearrangement using the equality $u_\alpha = -u_{1-\alpha}$

$$Z_{xy}[m] \leq \hat{Z}_{xy}[m] - \frac{1}{\sqrt{K-2}} + u_{1-\alpha} \tag{12}$$

6.2 Confidence Intervals of Coherence and *Z*-coherence

Confidence intervals of magnitude squared coherence estimate $|\hat{\gamma}_{xy}|^2$ cannot be computed directly, because these values are not of normal distribution. At first, it is necessary to compute *z*-coherence estimate $\hat{Z}_{xy}[m]$ using equation (7). Two-tailed confidence interval of magnitude squared coherence could be then evaluated from expression [4]

$$\begin{aligned} &\Pr\left\{\tanh^2\left[\frac{1}{\sqrt{K-2}}\left(\hat{Z}_{xy}[m] - \frac{1}{\sqrt{K-2}} - u_{1-\frac{\alpha}{2}}\right)\right] < \right. \\ &< |\gamma_{xy}[m]|^2 \leq \\ &\left. \leq \tanh^2\left[\frac{1}{\sqrt{K-2}}\left(\hat{Z}_{xy}[m] - \frac{1}{\sqrt{K-2}} + u_{1-\frac{\alpha}{2}}\right)\right]\right\} = 1-\alpha \end{aligned} \tag{13}$$

where $\Pr\{\}$ means probability of the event in curly brackets, K is a number of periodograms used for smoothing of PSDs, from which $\hat{Z}_{xy}[m]$ was computed, $|\gamma_{xy}[m]|^2$ represents the real value of magnitude squared coherence and $u_{1-\frac{\alpha}{2}}$ is a fractile of standard normal distribution $N(0,1)$.

For *z*-coherence, the computation of confidence intervals is analogical but easier because no reverse transformation is needed. The expression (13) switches to

$$\begin{aligned} &\Pr\left\{\hat{Z}_{xy}[m] - \frac{1}{\sqrt{K-2}} - u_{1-\frac{\alpha}{2}} < Z_{xy}[m] \leq \right. \\ &\left. \leq \hat{Z}_{xy}[m] - \frac{1}{\sqrt{K-2}} + u_{1-\frac{\alpha}{2}}\right\} = 1-\alpha \end{aligned} \tag{14}$$

where $Z_{xy}[m]$ is the real value of *z*-coherence. The use of equations (13), (14) is correct, only if the condition for coherence to *z*-coherence transformation is fulfilled, so if $K>20$.

Acknowledgements

The research was supported by the project of the Czech Ministry of Education MSM 6840770012 "Transdisciplinary Research in Biomedical Engineering 2", MSM 0021620816 and IGA NF 8232/3. We are grateful to Dr. Kozák and Dr. Vrba for providing patient volunteers and to Dr. Vrána and Dr. Poláček for their help during data recording.

References

[1] BENDAT, J. S., PIERSOL, A. G. *Random Data: Analysis and Measurement Procedures.* New York: John Wiley & Sons, 1971.

[2] BORTEL, R., SOVKA, P. Approximation of Statistical Distribution of Magnitude Squared Coherence Estimated with Segment Overlapping. *Signal Processing.* 2007, vol. 87, no. 5, pp. 1100–1117.

[3] KOZÁK, J. et al. Methodical Instructions for Acute and Chronic Non-Oncogenous Pain Pharmacotherapy (in Czech). *Bolest.* 2004, vol. 7, sup. 1, pp. 9–18.

[4] SVOBODA, L. *Detection of Electrocortical Rhythms Induced by Spinal Neurostimulator in Patients Suffering from Chronic Pain* (in Czech). Diploma thesis. Prague: FEE CTU, Dept. of Circuit Theory, 2006.

[5] SVOBODA, L., STANČÁK A., SOVKA, P. Detection of Cortical Oscillations Induced by SCS Using Power Spectral Density. *Radioengineering.* December 2007, vol. 16, no. 4.

[6] THICKBROOM, G. W. et al. Source Derivation: Application to Topographic Mapping of Visual Evoked Potentials. *Electroencephalography and Clinical Neurophysiology.* July 1984, vol. 4, no. 59, pp. 279–285.

About Author…

Lukáš SVOBODA – for biography see p. 45 of this issue.